Journal of Communicable Diseases
Volume 58, Issue 1 - 2026, Pg. No. 104-119
Peer Reviewed & Open Access Journal

Research Article

Prevalence, Proteomic Profiling and In Silico Allergenicity Prediction of Cytosolic Proteins of *Aspergillus fumigatus* Obtained from Respiratory Patients

Priya Koundal[1], Pawan Kumar[2], Vedika Sharma[3], Sunita Manhas[4], Shahbaz Aman[5], Shakeel Ahmed Mohammed[6], Kajal[7]

[1,4]Department of Biochemistry, Maharishi Markandeshwar Institute of Medical Sciences and Research, Maharishi Markandeshwar, Deemed to be University, Mullana-Ambala, Haryana, India
[2]Chaudhary Charan Singh Haryana Agricultural University, Hisar, India
[3]Department of Microbiology, Pt JLNGMCH, Chamba, Himachal Pradesh, India
[5]Department of Microbiology, Maharishi Markandeshwar Institute of Medical Sciences and Research, Maharishi Markandeshwar, Deemed to be University, Mullana, Ambala, Haryana, India
[6,7]Department of Biosciences & Technology and Central Research Cell, Maharishi Markandeshwar Engineering College, Maharishi Markandeshwar, Deemed to be University, Mullana-Ambala, Haryana, India
DOI: https://doi.org/10.24321/0019.5138.202615

I N F O

Corresponding Author:
Shahbaz Aman, Department of Microbiology, Maharishi Markandeshwar Institute of Medical Sciences and Research, Maharishi Markandeshwar, Deemed to be University, Mullana, Ambala, Haryana, India
E-mail Id:
shahbazaman095@gmail.com
Orcid Id:
https://orcid.org/0000-0002-9929-8534
How to cite this article:
Koundal P, Kumar P, Manhas S, Sharma V, Aman S, Mohammed S A, Kajal, Prevalence, Proteomic Profiling and In Silico Allergenicity Prediction of Cytosolic Proteins of *Aspergillus fumigatus* Obtained from Respiratory Patients. J Commun Dis. 2026;58(1):104-119.

Date of Submission: 2025-09-25
Date of Acceptance: 2026-02-28

A B S T R A C T

Introduction: Aspergillus fumigatus is a major opportunistic fungal pathogen associated with asthma, chronic obstructive pulmonary disease (COPD), and tuberculosis (TB), yet its burden is often underestimated, particularly where relapse cases are diagnosed without adequate fungal evaluation.

Materials & Methods: A total of 100 patients with COPD, asthma, and TB were recruited. Microbiological, serological, and radiological methods were used to identify *Aspergillus* co-infection. Isolates were assessed for siderophore production, followed by conidial protein extraction and SDS-PAGE. Proteins were characterized using Orbitrap LC-MS/MS. Allergenicity was predicted using AllerTOP, Allermatch, and Allergome, while epitope mapping was performed using IEDB, ABCpred, BCEpred, and NetMHC. A multi-epitope vaccine was designed and evaluated through structural modelling and docking with TLR2 and TLR4.

Results: A. fumigatus was isolated from COPD (7.9%) and TB (5.7%) patients. Elevated total IgE and specific IgG levels were observed in most cases. All isolates produced siderophores (mean halo 13 ± 1 mm), indicating virulence. Proteomic analysis identified 1,582 proteins, of which 198 were predicted allergens, including 14 cytosolic proteins such as enolase and malate dehydrogenase. Epitope prediction yielded seven B-cell, eight MHC-I, and four MHC-II epitopes, leading to the construction of a 314-amino-acid chimeric vaccine. The model showed stability, antigenicity, non-allergenicity, and strong binding affinity with TLR2 (−280.5 kJ/mol) and TLR4 (−280.7 kJ/mol).

Conclusion: This study provides comprehensive proteomic and immunoinformatic insights into *A. fumigatus*, identifying novel cytosolic allergens and proposing a structurally stable multi-epitope vaccine, offering a promising strategy for targeted immunotherapy against fungal co-infections.

Keywords: Asthma, COPD, Tuberculosis, co-infection, *A. fumigatus*, Respiratory Distress.

Introduction

Aspergillus, a fungus commonly distributed across various environmental habitats such as soil, decaying plant matter, and indoor air, thrives particularly in high-humidity conditions.[1] With a catalogue of more than 300 identified species, noteworthy among them being *A. fumigatus*, *Aspergillus flavus*, *Aspergillus* niger, and *Aspergillus* terreus, several have been recognised as pathogenic to humans. Among these, *A. fumigatus* stands out as the most well-known and frequently encountered pathogenic species, followed by *A. flavus*; however, *A. niger* and *A. terreus* also demonstrate virulence.[2] While *Aspergillus* infections typically do not pose a threat to healthy individuals, patients with chronic conditions such as asthma, COPD, or tuberculosis often have compromised immune systems, rendering them susceptible to acquiring *Aspergillus* infections. Respiratory tract illnesses such as *Aspergillus* bronchitis, *Aspergillus* pneumonia, and allergic bronchopulmonary aspergillosis (ABPA) may manifest following inhalation of *Aspergillus* spores.[3] Invasive aspergillosis infections in chronically ill patients can significantly elevate morbidity and mortality rates, leading to exacerbated symptoms, prolonged hospital stays, and potential fatality.[4] The surge in asthma incidence and prevalence is predominantly associated with industrialisation.[5] Inhalation of allergens, particularly *Aspergillus* spores, plays a pivotal role in eliciting airway inflammation in allergic asthma patients.[6] *A. fumigatus* is primarily linked to ABPA characterised by symptoms such as coughing, wheezing, and dyspnoea. It can incite allergic reactions in asthma patients, resulting in airway inflammation and constriction.[7] *Aspergillus* stimulates pattern recognition receptors, triggering cytokine activation and eliciting cellular and humoral immune responses.[8] The clinical spectrum of *Aspergillus*-associated hypersensitivity respiratory diseases encompasses *Aspergillus*-induced asthma, ABPA, and allergic *Aspergillus* sinusitis (AAS).[9] Understanding the frequency of *Aspergillus* sensitivity in asthmatic participants is crucial due to its association with the mould *Aspergillus*. Chronic obstructive pulmonary disease (COPD) patients with *Aspergillus* spp. growth in their airways are often stigmatised.[10] Although data on the prevalence of invasive pulmonary aspergillosis (IPA) in this population is lacking, mounting evidence suggests that individuals with severe COPD are at higher risk of infection.[11] Establishing a definitive diagnosis of IPA in COPD patients can be challenging, as tissue samples are rarely obtained before death. Diagnosis typically relies on radiographic evidence, clinical features, microbiological findings, and occasionally serological data.[12] Several factors, including prolonged exposure to irritants such as cigarette smoke, can precipitate chronic obstructive pulmonary disease (COPD), a progressive lung ailment characterised by breathing difficulties.[13] Allergic bronchopulmonary aspergillosis (ABPA) is a reaction to *Aspergillus* that can occasionally affect individuals with COPD. Symptoms of ABPA, if left untreated, can exacerbate and include wheezing, coughing, and dyspnoea.[14] Furthermore, tuberculosis (TB) patients face additional risks, including the development of chronic cavitary pulmonary aspergillosis (CCPA) and chronic fibrosing pulmonary aspergillosis (CFPA), complicating TB management and demanding tailored treatment strategies.[15] Asthma, COPD, and tuberculosis represent significant respiratory conditions with various implications for fungal infections, particularly those caused by *Aspergillus species*. Understanding the interplay between these respiratory diseases and fungal infections is crucial for effective management and improved outcomes in affected individuals. In the current study, the presence of *Aspergillus* co-infection has been studied by analysing clinical features of patients, radiographic evidence, and microbiological and serological findings among clinically diagnosed asthma, COPD, and tuberculosis patients.

Materials and Methods

Subject Recruitment and Ethics

Patients with a confirmed clinical diagnosis of asthma, COPD or tuberculosis were enrolled from the respiratory department at MMIMSR, Mullana, Ambala. Recruitment of study subjects was done after obtaining the approval from the institutional ethics committee. Furthermore, informed consent was also obtained from all the participants in compliance with Helsinki guidelines.[16,17]

Clinical Assessment

A comprehensive clinical assessment, including a detailed history and evaluation of respiratory manifestations such as dyspnoea, cough, wheezing, and sputum production, was obtained from each recruited participant. Data regarding underlying chronic respiratory conditions, smoking habits, corticosteroid therapy and use of alternative medicine were also obtained to evaluate the potential risk factors associated with fungal sensitisation or co-infection.[18]

Diagnosis of *A. fumigatus* Co-infection

Diagnostic Criteria

International Society for Human and Animal Mycology (ISHAM) guidelines were followed to diagnose the *Aspergillus* infection among enrolled participants.[18] Participants with at least elevated *A. fumigatus*-specific IgE & total IgE (major criteria) along with raised *A. fumigatus*

ISSN: 0019-5138
DOI: https://doi.org/10.24321/0019.5138.202615

IgG or eosinophilia or radiographic evidence (minor criteria) were considered positive for *A. fumigatus* infection.[19]

Skin Prick Test

0.5 ml of *A. fumigatus* antigen diluted at a ratio of 1:10 was injected superficially on the volar aspect of the forearm. Buffered saline & glycerinated histamine acid phosphate were also applied as negative & positive controls at a distance of 2.5 cm from the test site. The test response was evaluated after 60 min by observing erythema/wheal formation. A wheal measuring ≥3 mm was counted as positive.[20]

Serological Analysis

A blood sample was collected from recruited participants and transferred into a plain vial & EDTA vial. After that, total IgE was quantified using commercial sandwich ELISA kits.[18] while specific IgE (Abbexa Ltd) and IgG (ab247190) against *A. fumigatus* were measured via indirect ELISA.[21]

Fungal Isolation and Identification

Sputum samples were obtained using sterile, wide-mouth containers, collected on three occasions (at 72-hour intervals) to enhance fungal element recovery. Specimens were inoculated onto Sabouraud dextrose agar (SDA) slants and incubated at 37°C for 1–4 weeks.[22] Preliminary identification was performed via 10% potassium hydroxide (KOH) mount and lactophenol cotton blue (LPCB) staining.[23] Reference strain *A. fumigatus* ATCC 1022 was used for quality control.[24]

CAS-Agar Siderophore Assay

A modified Chrome Azurol S (CAS) assay was used for siderophore detection in fungal cultures. Petri plates were split in half, with one half containing malt extract agar (MEA) and the other half containing CAS-blue agar. Fungal inoculation occurred on MEA. After 6 days, at 28°C, colour change (blue to orange/purple) in CAS agar was measured in mm daily, and the rate was calculated as colour shift distance/incubation time.[25]

Fungal Protein Extraction

Clinical *A. fumigatus* isolates were maintained on SDA plates (HiMedia), and conidial protein extraction was performed as described by Carberry et al. (2006), with modifications as outlined by Singh et al. (2010).

Protein Quantification

Protein concentration (from fungal samples or cells) was determined using the bicinchoninic acid (BCA) assay. BSA standards were prepared (2 mg/mL) for calibration. Samples (2 µL + 23 µL water) and standards were mixed with 200 µL BCA reagent, incubated at 37°C for 30 min, and read at 562 nm.[26]

SDS-PAGE Protein Separation

Proteins (20 µg) were separated via 12.5% SDS-PAGE using the Laemmli protocol (27). Samples were denatured with Laemmli buffer (Tris-HCl, DTT, SDS, bromophenol blue, glycerol) at 95°C for 10 min and electrophoresed at 80 V, followed by Coomassie blue staining per previously established protocol to make the protein bands visible.[28]

Orbitrap LC-MS/MS and Proteomic Analysis

Purified protein samples were analysed via Orbitrap mass spectrometry. Peptide spectra were resolved using the Mascot algorithm (Matrix Science). Protein identification followed established workflows.[29]

Bioinformatics Screening

Allergenicity

The allergenicity prediction web tool AllerTOP v2 (https://www.ddg-pharmfac.net/allertop_test) and Allermatch (https://allermatch.org/allermatchsearch/form) were used to predict the allergenicity of selected proteins, harnessing physicochemical, motif, and structural attributes.[30] Proteins predicted to be allergenic were further evaluated for their allergenic profile using the Allergome tool (https://allergome.org/). The allergenic proteins that did not show any yeast allergens were selected for further epitope design.

Epitope Mapping

For the selected protein, B-cell and T-cell (MHC-I, MHC-II) epitopes were predicted using various online tools. Online tools such as IEDB (Immune Epitope Database) (http://tools.iedb.org/bcell/), ABCpred (https://webs.iiitd.edu.in/raghava/abcpred/ABC_submission.html), BCEpred (https://webs.iiitd.edu.in/raghava/bcepred/bcepred_submission.html), and those developed by Kolaskar and Tongaonkar.[31,32] were utilised to predict B-cell epitopes, while tools IEDB MHC class I tool (https://nextgen-tools.iedb.org/pipeline?tool=tc1), NetMHC 4.0 (https://services.healthtech.dtu.dk/services/NetMHC-4.0/), IEDB MHC class II tool (https://nextgen-tools.iedb.org/pipeline?tool=tc2), and NetMHC II 2.3 (https://services.healthtech.dtu.dk/services/NetMHCII-2.3/) were employed to predict MHC epitopes.[33,34] Consensus B-cell and T-cell epitopes from various tools were selected for designing a multi-epitope vaccine.

Multiepitope Vaccine Design

The amino acid sequence for human β-defensin 3 (hBD-3, 45 aa, UniProt Q5U7J2) was used as an N-terminal adjuvant.[35] using peptide linkers EAAAK. Selected MHC-I, MHC-II and B-cell epitopes were linked using specific peptide linkers (AAY, GPGPG, KK) to ensure proper folding and processing.[36,37] The designed multi-epitope underwent further in silico validation, using the Expasy ProtParam server (https://web.expasy.org/protparam/), Protein-Sol server (https://protein-sol.manchester.ac.uk/), ANTIGENpro server (https://scratch.proteomics.ics.uci.edu/), IEDB Immunogenicity server (http://tools.iedb.org/immunogenicity/), and PSIPRED, for stability, solubility, and non-allergenicity.[38]

ISSN: 0019-5138
DOI: https://doi.org/10.24321/0019.5138.202615

Structure modelling and validation

The tertiary structure of the predicted multi-epitope vaccine was modelled using various modelling tools, including AlphaFold (https://alphafoldserver.com/), PhyRe 2.2 (https://www.sbg.bio.ic.ac.uk/~phyre2/html/page.cgi?id=index), and D-I-TASSER (https://zhanggroup.org/D-I-TASSER/). The structure was validated using multiple criteria, including QMEAN score, ERRAT score, Verify3D and Ramachandran plot analysis. The best structure(s) were further refined using the Galaxy Refine server (https://galaxy.seoklab.org/cgi-bin/submit.cgi?type=REFINE) and validated.

Molecular docking

Molecular docking was employed to analyse the binding affinity between constructed multi-epitope vaccine candidates and immune receptors. PDB files for TLR2 (PDB ID: 6NIG) and TLR4 (PDB ID: 4G8A) were obtained from the RCSB PDB database. Both the files were prepared for docking by removing non-protein entities, including water and ions, followed by energy minimisation. The protein-protein docking of the multi-epitope construct with TLR2 and TLR4 was performed through the HDOCK server (http://hdock.phys.hust.edu.cn/). LigPlot + and PyMol were utilised to examine the interacting residues between the docked chains.

Results

Study Population

In the present study, a total of 100 subjects with respiratory illnesses were recruited from the Department of Respiratory Medicine at Maharishi Markandeshwar Institute of Medical Science and Research (MMIMSR), Mullana, Ambala, Haryana, India. Among these, 27 subjects were diagnosed with asthma, 38 with chronic obstructive pulmonary disease (COPD), and 35 with tuberculosis (TB). All participants were included in the study after obtaining clearance from the institute's ethical committee and providing written informed consent. The random distribution of subjects across these three respiratory illnesses ensured a diverse representation of patients, thereby allowing a comprehensive investigation into the prevalence and impact of *Aspergillus* species co-infection in these populations.

Prevalence of *Aspergillus* Species in Sputum Samples

Sputum samples collected from the study population were subjected to fungal culture analysis to identify *Aspergillus* species. Out of the 38 COPD patients, 6 yielded positive cultures for *Aspergillus* species, whereas among the 27 asthmatic patients, only one was culture-positive for *Aspergillus species*. In the tuberculosis group, 3 out of 35 patients showed culture positivity. Species-level identification revealed that 3 COPD patients were infected with *A. fumigatus*, 2 with *Aspergillus niger*, and 1 with *Aspergillus flavus*. Among TB patients, 2 were positive for *A. fumigatus*, while asthmatic patients showed only *A. flavus* colonisation. Notably, *A. fumigatus* was isolated exclusively from COPD and TB patients, suggesting a disease-specific predisposition to colonisation. Patients confirmed to have *A. fumigatus* co-infections were subsequently included in the detailed analysis of the study (Fig. 1).

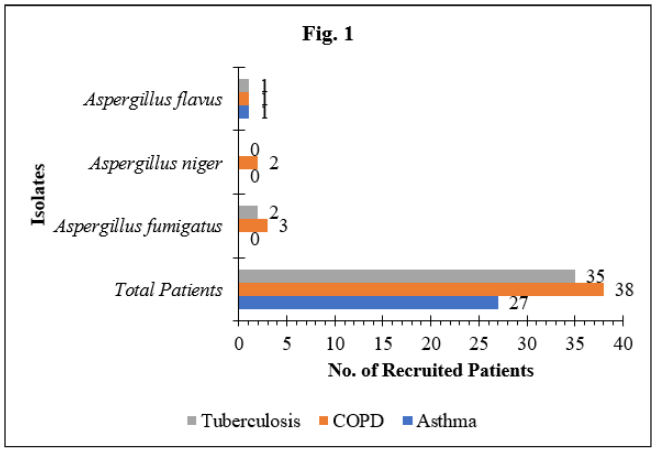

Figure 1.Distribution of Aspergillus species isolated from patients with different pulmonary diseases.

Clinical and Diagnostic Profiles of Co-infected Patients

A detailed analysis was carried out on five patients (S1, S2, S3, S4, and S5) with COPD and TB who were co-infected with *A. fumigatus*. The age of the patients ranged from 45 to 82 years, with a predominance of males. All patients exhibited common respiratory symptoms such as cough, breathlessness, and wheezing, which are indicative of respiratory distress. Radiological investigations, however, revealed distinct patterns between patients with COPD and those with TB. For instance, patient S1 presented with mucus plugging, whereas patient S2 showed infiltrative opacities in the right upper and mid zones. Patient S3 demonstrated infiltrative opacities in the left lower zone, while TB patients S4 and S5 showed infiltrative opacities in the right upper and mid zones and bronchiectatic changes in the bilateral lower zones, respectively. These radiological variations highlighted disease-specific pulmonary changes, with COPD patients showing patterns of chronic inflammation and airway obstruction, while TB patients exhibited granulomatous and fibrotic lesions (Table 1).

Skin Prick Test Findings

The skin prick test was performed to assess allergenic sensitisation among all recruited patients. The test revealed variable wheal sizes, suggesting differing allergen sensitivities. Patients S2 and S4 exhibited the largest wheal diameters of 21 mm each, followed by patient S5 with a wheal size of 20 mm. In contrast, patients S1 and

ISSN: 0019-5138
DOI: https://doi.org/10.24321/0019.5138.202615

S3 showed relatively smaller wheal sizes of 17 mm and 19 mm, respectively. The results indicated heightened allergen sensitivity in S2, S4, and S5, which may contribute to aggravated allergic responses in these patients compared to those with smaller wheal sizes.

Serological Findings and Culture Results

Serological evaluation included measurement of serum total IgE, *A. fumigatus*-specific IgE, and *A. fumigatus*-specific IgG. The reference ranges for these parameters are typically below 62 KU/L, 0.1 KU/L, and 27 KU/L, respectively. Four patients, namely S1, S2, S4, and S5, exhibited markedly elevated total IgE levels of 1760 KU/L, 309 KU/L, 1237 KU/L, and 751 KU/L, respectively, while patient S3 remained within the normal range at 61.40 KU/L. With respect to *A. fumigatus*-specific IgE, patient S2 had the highest level (0.8 KU/L), followed by S4 (0.6 KU/L), S1 (0.38 KU/L), and S5 (0.3 KU/L). Patient S3 showed negligible levels (0.01 KU/L). *A. fumigatus*-specific IgG was also elevated in patients S2 (66.8 KU/L), S4 (81.1 KU/L), and S5 (72.2 KU/L), whereas patients S1 (4.75 KU/L) and S3 (0.72 KU/L) demonstrated low levels. These findings confirmed four true positive patients (S1, S2, S4 & S5), while S3 was considered negative because it did not satisfy the major criteria. Elevated IgE and IgG levels indicated that fungal colonisation may contribute to exacerbated respiratory symptoms and complications in susceptible individuals.

Serum total protein levels were also assessed in the co-infected patients. All five patients demonstrated higher values compared to standard physiological ranges, with S1, S2, S3, S4, and S5 recording levels of 7 g/dL, 6.4 g/dL, 6.64 g/dL, 8.6 g/dL, and 6.5 g/dL, respectively. Parallel to serological findings, fungal cultures confirmed the growth of *A. fumigatus* in the respiratory tract samples, confirming active colonisation in these patients.

Clinical Significance of *A. fumigatus* Co-infection

The co-infection of COPD and TB patients with *A. fumigatus* was found to significantly complicate disease management. Radiological findings pointed to distinct disease-specific pulmonary involvement, while skin prick tests indicated allergen sensitivity in varying degrees. Serological markers highlighted both sensitisation and chronic infection, suggesting that *A. fumigatus* plays an important role in worsening respiratory function. The elevated total IgE and specific IgG levels indicated chronic exposure and immune activation, thereby increasing the likelihood of recurrent exacerbations, treatment complications, and hospitalisations. These findings emphasise the importance of routine epidemiological and incidence-based screening for *A. fumigatus* among patients with respiratory illnesses to ensure timely diagnosis and effective management strategies.

Table 1.Clinical & diagnostic findings of asthma, COPD and tuberculosis patients co-infected with *A. fumigatus*

Sample No.		S1	S2	S3	S4	S5
Age/Sex		82/M	61/F	70/M	45/M	60/M
Respiratory illness		COPD	COPD	COPD	Tuberculosis	Tuberculosis
Clinical symptoms	Cough	Yes	Yes	Yes	Yes	Yes
	Breathlessness	Yes	Yes	Yes	Yes	Yes
	Wheezing	Yes	Yes	Yes	Yes	Yes
X-Ray impression		Mucus plugging	Infiltrative opacities in the right upper and mid zone	Infiltrative opacities in the left lower zone	Infiltrative opacities in the right upper and mid zone	Bronchiectatic changes in the bilateral lower zones
Skin prick test (Wheal Size)		17 mm	21 mm	19 mm	21 mm	20 mm
Total IgE (Ref. Range: ≤ 62 KU/L)		1760	309	61.40	1237	751
A. fumigatus specific IgE (Ref. Range: ≤ 0.1 KU/L)		0.38	0.8	0.01	0.6	0.3
A. fumigatus specific IgG (Ref. Range: ≤ 27 KU/L)		4.75	66.8	0.72	81.1	72.2
Total Protein (Ref. Range: 4-6 g/dl)		7	6.4	6.64	8.6	6.5

ISSN: 0019-5138
DOI: https://doi.org/10.24321/0019.5138.202615

Absolute eosinophil count	02	01	04	06	05
Culture positive	Yes	Yes	Yes	Yes	Yes

Siderophore Production in Clinical Isolates of *A. fumigatus*

All four *A. fumigatus* clinical isolates produced siderophores on split MEA/CAS plates, evidenced by a progressive blue-to-orange/purple colour change in the CAS agar adjacent to fungal growth. On day 6 of incubation, distinct orange halos were clearly visible at the mycelial growth–medium interface, indicating active iron chelation. Quantitatively, the halo distances measured from the MEA–CAS interface were P1: 12.5 mm, P2: 13.0 mm, P3: 14.0 mm, and P4: 12.0 mm, corresponding to expansion rates of 2.08, 2.16, 2.33, and 2.00 mm/day, respectively. The cohort mean ± SD halo distance at day 6 was 12.9 ± 0.8 mm, yielding a mean production rate of 2.14 ± 0.13 mm/day; the median rate was 2.12 mm/day (range 2.00–2.33 mm/day). Normalising to colony radius to account for growth variation gave a mean halo-to-colony ratio of 1.12 ± 0.09, confirming robust, isolate-independent siderophore secretion. Overall, the pooled mean halo size measured approximately 13 ± 1 mm at day 6, corresponding to an average production rate of 2.16 mm/day, thereby confirming strong and consistent siderophore-producing potential among *A. fumigatus* isolates (Fig. 2).

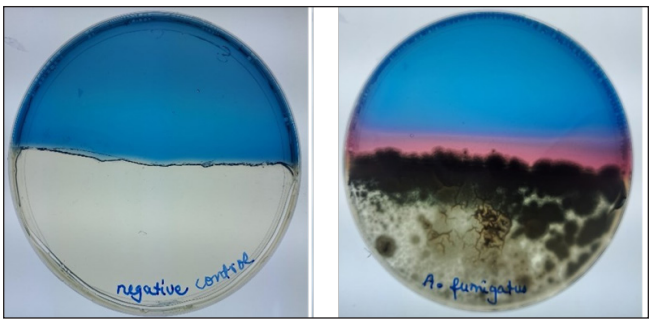

Figure 2.Detection of siderophore production by A. fumigatus by CAS-agar assay

Conidial Protein Quantification & SDS-PAGE Analysis

The BCA protein assay is an established method to quantify the amount of protein extracted from a given sample. Standard curve construction using BSA (0.39-25 µg/mL) achieved excellent linearity ($R^2 > 0.99$). Clinical isolate protein concentrations ranged from 5.27 to 9.90 mg/mL, confirming successful extraction of high-quality proteomic material. Electrophoretic separation of conidial proteins from four *A. fumigatus* isolates (S1-2, 4-5) revealed complex protein profiles with multiple bands spanning 10-250 kDa molecular weight ranges, indicating successful extraction of diverse protein populations suitable for mass spectrometric analysis (Fig. 3).

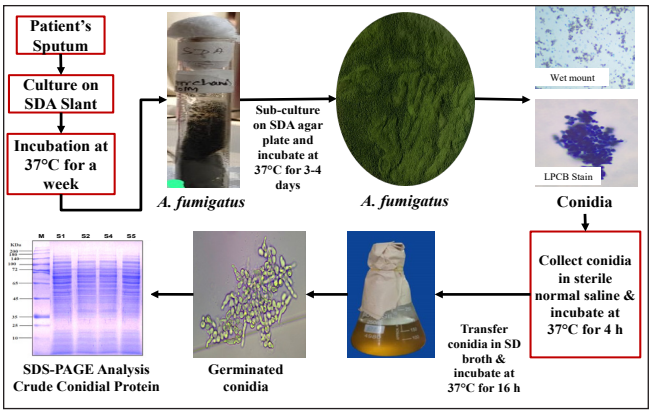

Figure 3.Isolation of *A. fumigatus*, extraction of conidial crude protein and SDS-PAGE analysis (M: Standard protein marker; S1, 2, 4 & 5: *A. fumigatus* Conidial Proteins)

Proteomic Profiling and

Comprehensive proteomic analysis of *A. fumigatus* clinical isolates using Orbitrap LC-MS/MS yielded 1,582 unique proteins, representing extensive coverage of the fungal proteome with high reproducibility across isolates S1, S2, S4 & S5, marking one of the most comprehensive *A. fumigatus* clinical isolate proteome datasets reported to date. Functional classification of these proteins revealed diverse categories, including metabolic enzymes involved in glycolysis, the TCA cycle, and amino acid metabolism; stress response proteins such as heat shock and oxidative stress regulators; cell wall biosynthesis machinery; virulence factors and pathogenicity determinants; as well as ribosomal and translation-related proteins.

Computational Allergenicity Prediction

Bioinformatics-driven allergenicity screening of 1,582 identified proteins was performed using online tools: AllerTOP v2.1 (an auto-cross-correlation function-based prediction tool), Allermatch (sequence similarity and cross-reactivity analysis), and ALLERGOME (a comprehensive allergen database comparison), which predicted 198 proteins (12.5% of the total proteome) to be allergenic (Supplementary File: S1). Among these, 14 proteins were localised in the cytosol (0.9% of the total proteome) (Table 2).

ISSN: 0019-5138
DOI: https://doi.org/10.24321/0019.5138.202615

Table 2.Allergen-Associated Cytosolic Proteins of *A. fumigatus* with Molecular Features and Clinical Relevance

Allergen Proteins	Accession	Sequence	AAs	MW [kDa]	Function	Clinical Significance
Catalase	A0A229YDB8	MATKIAGGLHRAQEVLQNTSSKSKKLVDLERDTADAHTQQPLTTDHGVRVSNTDQWLRVTNDRRTGPSLLEDQIAREKIHRFDHERIPERVVHARGTGAFGNFKLKESIEDLTYAGVLTDTSRNTPVFVRFSTVQGSRGSADTVRDVRGFAVKFYTDEGNWDIVGNNIPVFFIQDAVKFPDFVHAVKPEPHNEVPQAQTAHNNFWDFVYLHPEATHMFMWAMSDRAIPRSYRMMQGFGVNTFALVNKEGKRHFVKFHWIPHLGVHSLVWDEALKLGGQDPDFHRKDLMEAIDNKAYPKWDFAIQVIPEEKQDDFEFDILDATKIWPEDLVPLRVIGELELNRNVDEFFPQTEQVAFCTSHIVPGIDFTDDPLLQGRNFSYFDTQISRLGINWEELPINRPVCPVLNHNRDGQMRHRITQGTVNYWPNRFEAVPPTGTKGSGVGGGFTTYPQRVEGIKNRALSDKFREHHNQAQLFYNSMSEHEKLHMKKAFSFELDHCDDPTVYERLAGHRLAEIDLELAQKVAEMVGAPIPAKALKQNHGRRAPHLSQTEFIPKNPTIASRRIAIIIGDGYDPVAFTGLKTAIKAASALPFIIGTKRSAIYADGEDKTSSKGIIPDHHYDGQRSTMFDATFIPGGPHVATLRQNGQIKYWISETFGHLKALGATGEAVDLVKETLSGTLDVQVASSQSPEPVEWYGVVTAGGKQKPESFKESVQILKGATDFVGKFFYQISQHRNYQRELDGLASTIAF	750	84.6	Antioxidant enzyme	ROS protection
Catalase-peroxidase	Q7Z7W6	MTQDKCPFKEQSSQPNFAGGGTSNKDWWPDRLKLNILRQHTAVSNPLDADFDYAAAFNSLDYEGLKKDLRALMTDSQDWWPADFGHYGGLFIRMAWHSAGTYRVFDGRGGAGQGQQRFAPLNSWPDNVSLDKARRLLWPIKQKYGNKISWADLLILTGNVALESMGFKTFGFAGGRPDTWEADEATYWGRETTWLGNDARYAKGFSGSDKRGSLIADEESHKTTHSRELETPLAAAHMGLIYVNPEGPDGNPDPVAAAHDIRDTFGRMAMNDEETVALIAGGHTFGKTHGAAPADNVGKEPEAAGLEAQGLGWANKHGSGKGPHTITSGLEVTWTKTPTQWNNNFLEYLFKFEWELTKSPAGAHQWVAKNADEIIPDAYDASK	759	83.7	Dual function enzyme	Virulence factor
		KHKPTMLTTDLSLRFDPAYEKIARRFLEHPDQFADAFARAWFKLTHRDMGPRARYLGPEVPSEVLIWQDPIPAVNHPLVDASDIAALKDEILASGVPPRSFISTAWAAASTFRGSDKRGGANGARIRLAPQRDWEVNNQPWLREALSALEAVQSRFNARGDSKKVSLADLIVLAGCAAVEKAAQDAGHPIKVPFVPGRMDASQEETDVQSFNHMEPFADGFRNFAKGPARPRAEHYLVDKAQLLNLSAPEMTVLVGGLRVLNTNYDGSTHGVFTSRPGALTNDFFVHLLDMNTAWKDVGNGELFEGSDRKTGGKKWTATRADLVFGSNAELRAIAEVYASNDGDMKFVKDFVAAWNKVMNLDRFDLKGKQTIPARL				
Cytidine deaminase	B0YA90	METPSGLTIQELETLSSKAIAAKANAYCPYSKFRVGACVLTKAGEYIAGANIENVAYPVGTCAERVAFGTAIAAGHQDFKAVAVATDITPGASPCGMCRQFMREFTTPSFPVFMYDGQGNYAVRTMGEVSNFFIAHSFFHIAACLRSIAGN	151	16	Nucleotide metabolism	RNA editing
Enolase	B0Y763	MPISKIHARSVYDSRGNPTVEVDVVTETGLHRAIVPSGASTGQHEAHELRDGDKTQWGGKGVLKAVKNVNETIGPALIKENIDVKDQSKVDEFLNKLDGTANKSNLGANAILGVSLAVAKAGAAEKGVPLYAHISDLAGTKKPYVLPVPFQNVLNGGSHAGGRLAFQEFMIVPDSAPSFSEALRQGAEVYQKLKALAKKKYGQSAGNVGDEGGVAPDIQTAEEALDLITEAIEQAGYTGKIKIAMDVASSEFYKADVKKYDLDFKNPESDPSKWLTYEQLADLYKSLAAKYPIVSIEDPFAEDDWEAWSYFYKTSDFQIVGDDLTVTNPGRIKKAIELKSCNALLLKVNQIGTLTESIQAAKDSYADNWGVMVSHRSGETEDVTIADIAVGLRSGQIKTGAPCRSERLAKLNQILRIEEELGENAVYAGSKFRTAVNL	438	47.3	Glycolytic enzyme	Major allergen, cross-reactive
Formate Dehydrogenase	Q4WDJ0	MVLIRSLSRHLRRPATSFLSTKGTLSPTSSSPFRAASLGGSISGARTLTASANLQGKVLMVLYDGGEHAKQQPGLLGTTENELGLRKWIEEQGHTLVTTSDKDGENSTFDKELVDAEVIITTPFHPGYLTAERLAKAKKLKLAVTAGVGSDHVDLNAANKTNGGITVAEVTGCNVVSVAEHVVMTILALVRNFVPAHEQIRNGEWDVAAVAKNEFDLENKVVGTVAVGRIGERVLRRLKPFDCKELLYYDYQPLRPEVEKEIGCRRVENLEEMLAQCDVVTINCPLHESTRGLFNKELISKMKKGSWLVNTARGAIVVKEDVAEAVKSGHLRGYGGD	418	45.7	C1 metabolism	Oxidative stress

ISSN: 0019-5138
DOI: https://doi.org/10.24321/0019.5138.202615

		VWFPQPAPKDHPLRYVQGPWGGGNAMVPHMSGTSIDAQIRYAQGTKAILESYFSG RHDYKPEDLIVKDGDYVTKAYGQRQK				
Large Ribosomal Subunit Protein P2	Q9UUZ6	MKHLAAYLLLALAGNTSPSSEDVKAVLSSVGIDADEERLNKLIAELEGKDLQELIAE GSTKLASVPSGGAAAAAPAAAGAAAGGAAAPAAEEKKEEEKEESDEDMGFGLFD	111	11.1	Translation	Protein synthesis
Leucine Aminopeptidase 2	Q4X265	MTTVVNLPRDPNTLSNYNNWVSTHITANFDILFDQRKLAGNVIHRFRSTTDGESNHI ILDTNHLDIGSVKVNGQPSEWEYLPRLEPYGTPLKIKLDQGVKLNETIEVDISVQTT EKCTALQWLTPAQTSNKKHPYMFSQCQAIHARSIFPCQDTPDVKCTLDFNITSPLPVI ASGLPVRGSSEAPKSDGKTLYKFHQKVPIPSYLFALASGDISEAPIGPRSVVATSPDK LGECQWELEADTEKFINAIEKIVYPYVWGEYNVLILPPSFPYGGMENPIFTFATPSIIS KDRENIDVIAHELAHSWSGNLVTNASWEHFWLNEGWTTYLERRLRHGEPYRHFSA IIGWKALTDSVEHFGPEHDFTKLITNLKGMDPDDAFSSIPYEKGFNFLFHLENLVGK SKFDRFIPHYFNKYKGKSLDSYEFKSTILDFFKDDSDASTALNELDWDSWFYAPGLP PKPDFDTSLVDVVYDLAKKWLSLPKSSFKPQPEDIRGLTANQVVVFLEQILVSERQL TPELSKLMGEIYGLAASQNIEVANLYFQVGLQAGDASVVEPTADLLGKIGRMKFVR PLYRKLAKFDRKRALDTFEKHKGFYHPICRAMVEKDLFGKKDE	614	69.7	Protease	Protein processing
Malate Dehydrogenase	B0YCS8	MVKAAVLGASGGIGQPLSLLLKACPLVDELALYDVVNTPGVAADLSHISSVAKVSG YLPKDDGLKNALTGTDIVVIPAGIPRKPGMTRDDLFKVNAGIVRDLVTGIAQYCPK AFVLIISNPVNSTVPIAAEVLKKQGVFDPKRLFGVTTLDIVRAETFTQEYSGQKDPS KVQIPVVGGHSGETIVPLFSKASPALDIPADKYDALVNRVQFGGDEVVKAKDGAGS ATLSMAYAGFRFAEKVIRASQGQSGIVEPTYIYLRGVTGGEEIANETGVEFFSTLVEL GRNGAEKAINILQGVTEQEKKLLEACTKGLKGNIEKGIEFVKNTPPK	330	34.8	TCA cycle enzyme	Metabolic allergen
Phosphoglycerate kinase	Q4WT69	MSLTNKLAITDVDLKDKRVLIRVDFNVPLNEKKEVTNPQRIVGALPTIKYAIEQGAK AVVLMSHLGRPDGKKNPKYSLKPVVPELEKLLGKSVIFTEDCVGKEVEETVNKAS GGQVILLENLRFHPEEEGSYKDEEGKKVKADKEKVAEFRKGLTALGDIYINDAFGT AHRAHSSMVGVDLPQKASGFLVKKELEYFAKALESPSRPFLAILGGSKVSDKIQLID NLLPKVNSLIITGGMAFTFKKTLENVKIGNSLFDEAGSKTVGDIIEKAKKNNVKIVL PVDYITADKFSADAKTGYATDEEGIPDGYMGLDVGDKSVKLYKETIAEAKTILWNG PPGVFEMEPFANGTKQTLDAAVDAAKNGAIVIIGGGDTATVAAKYGAEEKLSHVST GGGASLELLEGKELPGVAALSSK	417	44.7	Glycolytic enzyme	Energy metabolism
Pyruvate Decarboxylase	B0YDT5	MDSDTLPLAQYLFKRLRQLGVDSIFGVPGDYNLTLLDHVVPSGLKWVGNCNELNA GYAADGYSRIKGIGALVTTFGVGELSAVNAIAGAYAERAPVVHIVGTPMRASQESR AMIHHTFIDGEYQRFDRMQEHVTVAQVSLSDHRTAPAEIDRILLQCLLHSRPVRITIP VDMVPVLVPTAGLASKIEIPPPVRQPQVEEAALTAVLERIYNAKKPMILVDGETRAF GTVNEVNQFVTTTGWPTFTSGFGKGLVDETLPNVYGVYRPAHKEFVDSCDLVLAF GPHFSNTNTYIFMVRPQDETSVLFNPTSVQVNKDIYRDLPAKYFIQQLTQRLDPSKIP VHQHNLVHPSAQVLPEVPPTDLVTQTAGFWRRLSPFFRSGDIVLGETGTPGYGAND FVLPPQTRLFKPVTWLSIGYMLPATLGASYAQRDLIARNEYHNLSAARTILFIGDGSF QMTVQELSTIIHHKLDVIVFLINNDGYTIERCIHGRNQAYNDVARWRYLKAPELFGA DQEGEYASRTWEIRTWADCDAVLKDEQLVNGKGLRMVEVFMDKFDAPDVLMNLL NAQIARDNAKK	575	64.1	Fermentation enzyme	Anaerobic adaptation
S-methyl-5'-thioadenosine phosphorylase	A0A8H4HLF3	MLGFSSLRRYLSSFTTRPLRRIESAKQLAKTMTVLPNTYDEPVRIAVIGGTGLRELPG FTQVASLSITTPWGSPSSPITILHHQCSHNNKTVAVAFLSRHGTHHQIAPHEVPARANI AALRSIGVRTIIAFSAVGSLQEEIKPRDFVIPDQVIDRTKGVRPWTFFEGGVVAHVPF GDPFDEGVAKVVRACGHSLEGEGVVLHDRGTLICMEGPQFSTRAESNLYRSWGGS VINMSCLPEAKLAREAEIAYQMICMSTDYDCWHESTADVTVEMVMGHMKANAQN	342	37.6	Methionine salvage	Nucleotide metabolism

ISSN: 0019-5138
DOI: https://doi.org/10.24321/0019.5138.202615

		ARRFVTAVLDALASDEHADLVQAKHVEGSIKFGLSTAQANWSPEARAKLEWLFPG YWN				
Uncharacterized Protein	A0A229XLH9	MSGMTPVFTTGACPPAGPYSQAIRANGQLFISGQIPADASGNLVEGNIGEKTQACCN NIKAILDAAGSSVDKIVKVNVFLTNMADFAEMNATYEKFFTHKPARSCVAVAQLPK GVPVEIECIALQ	125	13.1	Unknown function	Novel allergens
Uncharacterized protein	A0A229XUP0	MAQTIRIPIRTEKAPLPPPFLSQGIKVGNMIYCSGQVGVDPTTGKMVEGPIQARTKQI LHNLSAVLEAGGSSLQDVVKVNIFLADMGDFAAVNEVYQAAFGEPKPARTCVAVK TLPLGTDVEIECSAVVTGVATVRDSRL	140	14.8	Unknown function	Novel allergens
Uncharacterized Protein	A0A229WFX8	MGFTDFVSEAGLTLANNYLASRSYVVGDAPSQADVVTFKAFSGAPDAEKYPHVAR WYKHIASFEPEFASLPGDASKAYTAYGPESTELPTNPKDKPAEDDDDMDLFGSDEEE EDPEVVAQREARLAEYKKKKEGKAKPAAKSIVTLEVKPWDDETNLDELLENVKAI EIDGLVWGAYKWVPVGFGIKKLQINLVVEDEKVSLDELQQRIEEDEDHVQSTDIAA MQKL	227	25.2	Unknown function	Novel allergens

B-cell and T-cell epitope mapping

Predicted 14 allergenic proteins were further used for the identification of epitopes. Common B-cell epitopes predicted through IEDB and ABCpred, with a score of 0.95, were selected for each allergenic protein (Supplementary File: S2). A total of 7 highly efficient B-cell epitopes (IQAAKDSYAD, VYDSRGNP, GGSISGA, DEIIPDAYDASHKP, GRPDGKKNP, HHQIAPHEVPAR, and LGETGTPGYGAN) were selected. For MHC-1, the NetMHC tool was used, and a total of 8 epitopes (IANETGVEF, FPQTEQVAF, RLAEIDLEL, YLFKFEWEL, ATYEKFFTHK, ILWNGPPGV, TPSFPVFMY, and SQADVVTFK) were predicted with a high confidence score of > 0.9. Similarly, MHC-II was predicted through the NetMHC-II web server, and only four highly confident epitopes (YCPKAFVLIISNPVNST, KELLYYDYQPLRPEV, GKKETATRADLVFGS, and LANNYLASRSYVVGD) were selected with a score of >0.9 (Supplementary File: S3).

Multiepitope Vaccine Construct

A multiepitope vaccine was designed by adding a human β-defensin 3 adjuvant(GIINTLQKYYCRVRGGRCAVLSCLPKE-EQIGKCSTRGRKCCRRKK) to the N-terminus, followed by an EAAAK linker - (MHC-I joined using AAY linkers), a GPGPG linker (MHC-II joined using GPGPG linkers) , and a KK linker (B-cell epitope joined using KK linkers). The CTL (MHC I) epitope region was formed of 94 aa, followed by helper T-cell (MHC II) epitopes, which consist of 77 aa, and the linear B-cell epitope region consists of 86 aa. Combined, all these formed a multiepitope construct of 314 aa (Table 3).

Computational analysis using the ProtParam server indicates a basic isoelectric point (>9) and an instability index of <40, suggesting a stable and soluble protein. Antigenicity prediction using the VaxiJen v2.0 server gave a score above the 0.5 threshold, and AllerTOP/AlgPred predicted the construct to be non-allergenic.[33,39,40] Therefore, the multi-epitope construct is expected to stimulate both arms of the adaptive immune system. Epitope-based designs that rationally combine dominant B-cell and T-cell epitopes can elicit a more efficient and specific immune response than whole antigens.[41] The inclusion of hBD-3 should further enhance immunogenicity by activating innate immune receptors (TLR1/2) and recruiting immune cells to the site of immunisation.[42] These features, combined, promote a balanced Th1/Th2 response with robust antibody production and cytotoxic T-cell activation while avoiding the risks associated with live vaccines.[41,42]

Table 3.Components and Predicted Sequences Used in the Multi-Epitope Vaccine Construct Design

Component	Details / Prediction Method	Amino Acid Sequence
Adjuvant (β-defensin 3)	Human β-defensin 3 (hBD3) sequence	GIINTLQKYYCRVRGGRCAVLSCLPKEEQIGKCSTRGRKCCRRKK
B-cell Epitope	Predicted using IEDB and ABCpred (Score > 0.95)	IQAAKDSYADKKVYDSRGNPKKGGSISGAKKDEIIPDAYDASKKHKPKKGRPDGK-KNPKKHHQIAPHEVPARKKLGETGTPGYGAN
MHC Class I Epitopes	Predicted using NetMHC/IEDB (Score > 0.9)	IANETGVEFAAYFPQTEQVAFAAYRLAEIDLELAAYYLFKFEWELAAYATYEKFFTH-KAAYILWNGPPGVAAYTPSFPVFMYAAYSQADVVTFK

ISSN: 0019-5138
DOI: https://doi.org/10.24321/0019.5138.202615

MHC Class II Epitopes	Predicted using NetMHCII/IEDB (Score > 0.9)	YCPKAFVLIISNPVNSTGPGPGKELLYYDYQPLRPEVGPGPGGKKWTATRADLVFGSGPGPGLANNYLASRSYVVGD
Multiepitope Construct	Final chimeric vaccine sequence (314 aa)	GIINTLQKYYCRVRGGRCAVLSCLPKEEQIGKCSTRGRKCCRRKKEAAAKIANETGVEFAAYFPQTEQVAFAAYRLAEIDLELAAYYLFKFEWELAAYATYEKFFTHKAAYILWNGPPGVAAYTPSFPVFMYAAYSQADVVTFKGPGPGYCPKAFVLIISNPVNSTGPGPGKELLYYDYQPLRPEVGPGPGGKKWTATRADLVFGSGPGPGLANNYLASRSYVVGDKKIQAAKDSYADKKVYDSRGNPKKGGSISGAKKDEIIPDAYDASKKHKPKKGRPDGKKNPKKHHQIAPHEVPARKKLGETGTPGYGAN

Multiepitope structure modelling and validation

The tertiary structure of the designed multiepitope vaccine was predicted using multiple ab initio-based modelling tools, including AlphaFold, PhyRe, and I-TASSER. The best model generated by AlphaFold showed a QMEAN score of -9.44, an ERRAT score of 83.871, and a Verify 3D score of 28.34. Additionally, Ramachandran plot analysis revealed that 80.7% of residues fell within the favoured region. However, the best model generated from I-TASSER showed a QMEAN score of -7.85, an ERRAT score of 68.3849, and a Verify 3D score of 90.45, with Ramachandran plot analysis indicating that 74.4% of residues fell within the favoured region. The model generated from the PhyRE server yielded a QMEAN score of -10.10, an ERRAT score of 43.4483, and a Verify 3D score of 23.25. Additionally, Ramachandran plot analysis revealed that 90.6% of residues fell within the favoured region.

The best model observed from AlphaFold and iTasser was further refined using the Galaxy Refine server. Among these, the iTasser model was observed to have a QMEAN score of -2.56, an ERRAT score of 81.9672, and a Verify 3D score of 92.36, with Ramachandran plot analysis indicating that 84.3% of residues fell within the favoured region, while 13.8% of residues were within the allowed region.

Molecular docking

To analyse the binding affinity between the constructed multi-epitope vaccine candidates and the immune receptors TLR2 and TLR4, molecular docking studies were performed using the HDOCK server. Both dock complexes exhibited more than 100 docking conformations, involving different binding sites of the constructed multi-epitope vaccine, with a binding energy of -280 kJ/mol for the optimal docking conformation. The top 5 docking conformations of TLR2 with the multi-epitope showed strong binding interactions (Table 4). Different binding conformations showed involvement of various B-cell and T-cell epitopes in binding with TLR2 (Fig. 4). The best dock conformation (first) had a dock score of -280.5 kJ/mol and a confidence score of 0.931, involving hydrogen bonds with MHC-I epitope YLFKFEWEL (Trp93-Arg63), MHC-II epitope YCPKAFVLIISNPVNST (Thr166-Tyr109), and B-cell epitope DEIIPDAYDASKKHKP (Lys274-Pro320, Lys272-Tyr323). The second dock conformation showed a total of 16 hydrogen bonds between TLR2 and epitopes, including MHC-I epitopes FPQTEQVAF (Glu67-Ser56), RLAEIDLEL (Arg75-Glu180, Glu78-Arg230, and Glu78-Arg257), and ATYEKFFTHK (Lys103-Asp58, and His107-Asp106), and the MHC-II epitope LANNYLASRSYVVGD (Val224-Arg447). The third dock conformation exhibited hydrogen bonds with MHC-II epitope YCPKAFVLIISNPVNST (Tyr150-Asn487), KELLYYDYQPLRPEV (Tyr177-Asn467, Tyr177-Arg486, Asp178-Asn468), and GKKETATRADLVFGS (Ser206-Arg447), as well as B-cell epitope HHQIAPHEVPAR (His289-Asp286, His290-Asn258, and His295-Arg321). The fourth dock complex involved hydrogen bonds with MHC-I epitopes TPSFPVFMY (Tyr132-Leu371), SQADVVTFK (Asp139-His318), and MHC-II epitopes YCPKAFVLIISNPVNST (Lys153-His398, Ala154-His398), KELLYYDYQPLRPEV (Tyr177-His426, Asp178-Ser424, Asp178-Arg447), and B-cell epitope IQAAKDSYAD (Asp234-Arg316). The fifth conformation displayed hydrogen bonds with MHC-I epitope, YLFKFEWEL (Glu94-Arg321), ILWNGPPGV (Gly119-Lys347), and MHC-II epitopes, KELLYYDYQPLRPEV (Tyr177-His426 and Arg183-Glu375). Overall, most of the predicted epitopes in the multiepitope construct showed hydrogen bond interactions with TLR2.

The best dock complex of TLR4 and the multiepitope construct yielded a dock score of -280.7 kJ/mol, accompanied by a confidence score of 0.932. The binding site analysis revealed the binding of different epitope constructs at various locations of TLR4 (Fig. 5). The first and best dock conformation showed TLR4 binding within the MHC-II epitope KELLYYDYQPLRPEV, at positions Arg183-Glu485, Tyr176-Asn486, Arg183-Asn486, and Tyr176-Glu509. The second-best dock conformation showed hydrogen bonding with the MHC-I epitopes YLFKFEWEL (Trp93-Thr106, Glu94-Ser105, Glu94-Thr106), ATYEKFFTHK (Lys108-Thr357, Lys108-Asp379), and SQADVVTFK (Gln137-Asp379, Gln137-Ser381, Gln137-Asp405, Asp139-Arg382), as well as with MHC-II epitopes YCPKAFVLIISNPVNST (Thr166-Pro28) and KELLYYDYQPLRPEV (Asp178-Arg264). The third dock conformation showed hydrogen bond interactions with one MHC-I epitope, ATYEKFFTHK (Glu102-Arg606) and two MHC-II epitopes, YCPKAFVLIISNPVNST (Tyr150-Gly480 and Lys153-

ISSN: 0019-5138
DOI: https://doi.org/10.24321/0019.5138.202615

His529) and KELLYYDYQPLRPEV (Tyr176-His458 and Tyr177-Ser482). The fourth dock conformation showed hydrogen bonds with two MHC-II epitopes: YCPKAFVLIISNPVNST (Tyr150-Thr499) and KELLYYDYQPLRPEV (Glu173-His426, Tyr176-Lys477, Tyr177-Val524, Arg183-His426, Arg183-Asp428, Arg183-Tyr451), along with a single hydrogen bond interaction with a B-cell epitope, VYDSRGNP (Tyr242-Gln39). The fifth dock conformation showed hydrogen bonds with MHC-I epitopes ATYEKFFTHK (Tyr98-Lys477, Glu102-Lys477, Lys103-Glu474) and TPSFPVFMY (Tyr132-Asp550, Tyr132-Asn575), and all MHC-II epitopes formed hydrogen bonds. In conclusion, most of the T-cell epitopes were involved in hydrogen bond interactions with TLR4, while B-cell epitopes engaged in other non-bonding interactions.

Table 4.Binding interactions between the multi-epitope vaccine and TLR

Sr. No.	TLR2		TLR4	
	Docking Score (kJ/mol)	Confidence Score	Docking Score (kJ/mol)	Confidence Score
1	-280.5	0.931	-280.7	0.932
2	-279.5	0.930	-278.9	0.929
3	-278.0	0.928	-278.5	0.929
4	-275.7	0.925	-277.9	0.928
5	-264.8	0.909	-277.9	0.928

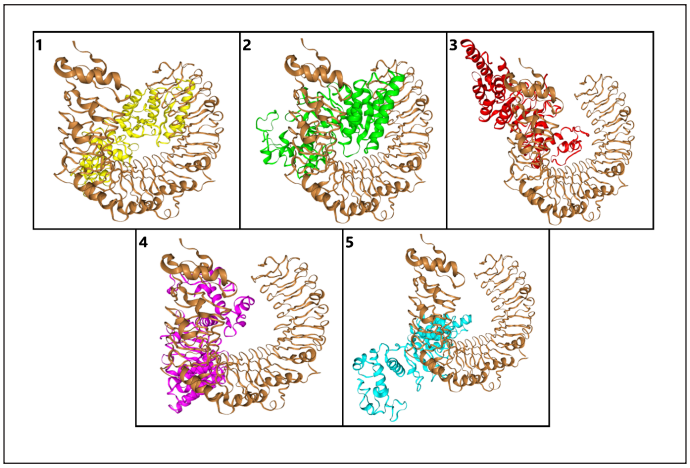

Figure 4.The dock conformation of TLR2 (grey colour) and the multi-epitope vaccine construct (in colours)

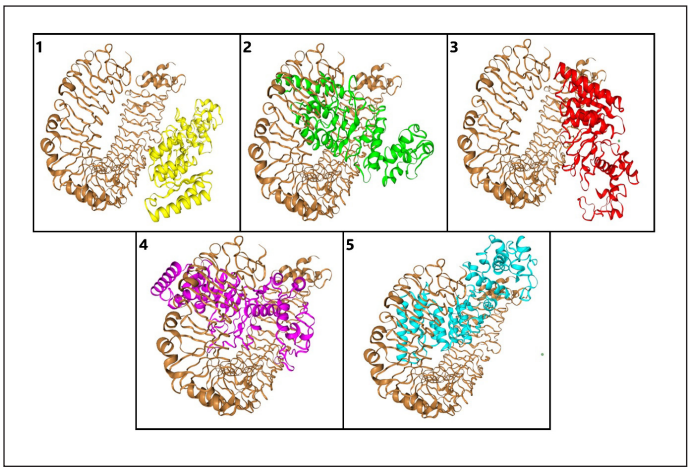

Figure 5.The dock conformation of TLR4 (grey colour) and the multi-epitope vaccine construct (in colours)

ISSN: 0019-5138
DOI: https://doi.org/10.24321/0019.5138.202615

Discussion

Chronic respiratory symptoms often persist despite appropriate treatment, suggesting that secondary or co-infections may contribute to disease progression. In regions with high tuberculosis prevalence, patients previously treated for pulmonary TB who develop recurrent respiratory symptoms are frequently misdiagnosed with relapse even when microbiological tests are negative, pointing toward possible co-infection. Increasing evidence links *Aspergillus* sensitisation with worsening COPD, asthma and tuberculosis. This connection likely arises from persistent mucus retention that promotes fungal colonisation and genetic susceptibilities such as surfactant protein A2 defects. According to the ISHAM, the global prevalence of *Aspergillus* sensitisation among asthmatics ranges from 5.5% to 38.5%, underscoring its significance in chronic respiratory disease.[20,43,46] In this study, microbiological analysis revealed the presence of *A. niger, A. fumigatus* & *A. flavus* among patients with respiratory illness and *A. fumigatus* being the most prevalent species. This finding is consistent with previous studies reported *A. fumigatus* as a common fungal pathogen among TB & COPD patients highlighting its role in exacerbating respiratory symptoms and contributing to disease progression.[47,48] Furthermore, the distribution of *Aspergillus species* varied across different respiratory illness besides *A. fumigatus* other species including *A. niger* and *A. flavus* were also identified. This diversity reflects how underlying lung diseases and host immunity can shape the fungal community within the airways in chronic respiratory disorders.[49] Clinical profiling of co-infected patients revealed distinct radiological patterns across asthma, COPD, and TB, reflecting underlying pathology and disease severity. These findings align with previous reports describing emphysematous and airway wall changes in COPD and granulomatous lesions in TB, underscoring the clinical impact of *Aspergillus* co-infection on respiratory health.[50,52] Furthermore, serological analysis revealed variations in sensitivity to allergens and elevated levels of total IgE, *A. fumigatus-specific* IgE, and IgG antibodies among co-infected patients. This aligns with another study that reported that patients with chronic respiratory diseases often exhibit elevated levels of specific IgE antibodies to *Aspergillus* antigens, indicating sensitisation to fungal allergens and potential exacerbation of respiratory symptoms.[53] The co-infection of *A. fumigatus* poses significant challenges in the management of respiratory illnesses, exacerbating symptoms and increasing the risk of recurrent exacerbations and hospitalisations.[54] The chronic nature of *A. fumigatus* infection further complicates long-term management, emphasising the importance of early detection and targeted interventions.[55] The robust and consistent siderophore production observed among all four clinical isolates of *A. fumigatus,* with a pooled mean halo size of approximately 13 mm and production rate of 2.16 mm/day, aligns well with recent research demonstrating reliable synthesis and secretion of key extracellular siderophores, such as triacetylfusarinine C and ferricrocin, during active growth, regardless of drug resistance or strain variability. This consistency in siderophore production underpins the fungus's capacity for iron acquisition, a requirement for virulence and infection in humans, and supports the use of siderophore quantitation as a sensitive, phase-dependent biomarker for discriminating invasive aspergillosis, particularly since mammalian cells do not produce these molecules, thus minimising false positives in diagnostic assays.[56,59] The comprehensive proteomic analysis of *A. fumigatus* clinical isolates in this study identified 1,582 unique proteins with high reproducibility across isolates S1, S2, S4, and S5, marking one of the most extensive clinical proteome datasets reported to date. Functional classification revealed diverse protein categories spanning metabolic enzymes, stress response proteins, cell wall biosynthesis machinery, and virulence factors, reflecting the complex biology and pathogenic potential of *A. fumigatus*. These findings correspond well with recent studies reporting similar proteomic coverage and functional diversity, such as proteomic characterisations that highlighted metabolic flexibility, oxidative stress regulation, and cell wall remodelling as key survival and virulence strategies in clinical isolates. For example, the 2024 study on *A. fumigatus* clinical proteomes similarly underscored the abundance of heat shock proteins and metabolic enzymes, further validating the biological relevance of our dataset. Likewise, investigations into the fungal secretome and surface proteomes have emphasised the importance of cell wall and extracellular proteins as virulence and immune-interaction determinants, corroborating our identification of these functional groups.[60,63] Bioinformatics-driven allergenicity screening in our study identified 198 proteins (12.5% of the total proteome) as potential allergens, including 14 cytosolic proteins and a refined set of high-confidence allergens predicted by multiple algorithms, thereby increasing prediction reliability. This prevalence of putative allergens is consistent with values reported in other computational allergenicity analyses of *A. fumigatus* proteomes, which typically identify between 10% and 15% of proteins as allergenic candidates. Research emphasising the sustainability of allergen prediction highlights proteases and cell wall-associated proteins as dominant allergens, aligning with our dataset's functional allergen profile. Similar studies, which validate allergenic determinants independent of isolate variation, reinforce the robustness of computational tools in identifying fungal allergens critical for host-pathogen interactions.[60,64,65] Moving to the multiepitope vaccine construct, our design comprises 314 amino acids, including the 45-aa human β-defensin 3 (hBD-

ISSN: 0019-5138
DOI: https://doi.org/10.24321/0019.5138.202615

3) adjuvant linked with CTL, helper T-cell, and B-cell epitopes. Computational analysis suggests good stability (instability index < 40), solubility, a basic isoelectric point (> 9), strong antigenicity (VaxiJen score > 0.5), and non-allergenicity (AllerTOP/AlgPred), making it a promising vaccine candidate. This rational epitope-based design aligns with recent vaccine development trends, favouring multi-epitope constructs over whole antigens to promote broad and balanced immune responses while minimising allergenic and adverse effects, a strategy increasingly supported in fungal vaccine research. The inclusion of hBD-3 as an immune-stimulatory adjuvant further enhances immunogenicity by activating innate immune receptors such as TLR1/2, a mechanism gaining traction in immunotherapy against fungal infections, as recent studies demonstrate improved vaccine efficacy and immune cell recruitment through a similar innate-adaptive immune interface targeting. These vaccine design principles align closely with recent computational and experimental research, which confirms that precise epitope mapping, combined with adjuvant usage, can yield safer and more effective vaccines against *Aspergillus* and other fungal pathogens.[66,68] Further molecular docking studies against TLR2 and TLR4 showed a good binding affinity of the designed multi-epitope. Taken together, our findings underscore the clinical significance of *A. fumigatus* as a significant opportunistic pathogen in patients with pre-existing respiratory conditions, such as asthma, COPD, and tuberculosis. The detection of *A. fumigatus* and other *Aspergillus* species in sputum samples, alongside corroborative radiological, serological, and allergological evidence, highlights the underestimated burden of aspergillosis in high TB-prevalence regions where relapse diagnoses are often made without sufficient fungal evaluation. The consistent siderophore production observed across isolates further underscores the organism's robust virulence strategies, which may serve as potential diagnostic biomarkers. Comprehensive proteomic profiling provided deep insights into the metabolic adaptability, virulence, and allergenic potential of *A. fumigatus*, with in silico allergenicity predictions strengthening the identification of clinically relevant allergens. Finally, the rational design of a multi-epitope vaccine construct exemplifies the translational potential of proteomics-driven computational pipelines in generating novel therapeutic candidates against fungal infections.

Conclusion

This study offers the first in-depth proteomic and immunoinformatic characterisation of *A. fumigatus* clinical isolates from Indian respiratory patients, establishing it as the predominant *Aspergillus* species co-infecting individuals with COPD and TB, with additional sensitisation observed among asthmatic cohorts. Clinical, immunological, microbiological and radiological evidence underscores the need for routine fungal screening among patients with chronic respiratory illnessess. The large-scale proteomic dataset generated provides a comprehensive catalogue of the *A. fumigatus* proteomee revealing novel cytosolic allergens of diagnostic and therapeutic importance. Comprehensive proteomic mapping, coupled with allergenicity profiling, identified 14 cytosolic allergens, including previously uncharacterised proteins. These findings deepen the understanding of *A. fumigatus* host interactions and provide a structural framework for developing precision immunotherapies or fungal diagnostics. Furthermore, this study is limited by its dependence on *in silico* analyses and a modest number of culture-positive isolates, highlighting the need for experimental validation of the predicted allergens. Future research should include functional assays and in-vivo analysis, including animal model, for its reliability as diagnostic or therapeutic biomarkers for *A. fumigatus*-associated respiratory diseases.

References

1. Paulussen C, Hallsworth JE, Álvarez-Pérez S, Nierman WC, Hamill PG, Blain D, Rediers H, Lievens B. Ecology of aspergillosis: insights into the pathogenic potency of Aspergillus fumigatus and some other Aspergillus species. Microbial biotechnology. 2017 Mar;10(2):296-322.
2. Arastehfar A, Carvalho A, Houbraken J, Lombardi L, Garcia-Rubio R, Jenks JD, Rivero-Menendez O, Aljohani R, Jacobsen ID, Berman J, Osherov N. Aspergillus fumigatus and aspergillosis: from basics to clinics. Studies in mycology. 2021 Sep 1;100(1):100115-.
3. Guo L, Wu X, Wu X. Aspergillus infection in chronic obstructive pulmonary diseases. The Clinical Respiratory Journal. 2023 Mar;17(3):129-38.
4. Xu Y, Shao M, Liu N, Tang J, Gu Q, Dong D. Invasive pulmonary aspergillosis is a frequent complication in patients with severe fever with thrombocytopenia syndrome: a retrospective study. International Journal of Infectious Diseases. 2021 Apr 1;105:646-52.
5. Molnár D, Gálffy G, Horváth A, Tomisa G, Katona G, Hirschberg A, Mezei G, Sultész M. Prevalence of asthma and its associating environmental factors among 6–12-year-old schoolchildren in a metropolitan environment—a cross-sectional, questionnaire-based study. International Journal of Environmental Research and Public Health. 2021 Dec 20;18(24):13403.
6. Furlong-Silva J, Cook PC. Fungal-mediated lung allergic airway disease: The critical role of macrophages and dendritic cells. PLoS pathogens. 2022 Jul 14;18(7):e1010608.
7. Lattanzi C, Messina G, Fainardi V, Tripodi MC, Pisi G, Esposito S. Allergic bronchopulmonary aspergillosis in children with cystic fibrosis: An update on the

ISSN: 0019-5138
DOI: https://doi.org/10.24321/0019.5138.202615

newest diagnostic tools and therapeutic approaches. Pathogens. 2020 Aug 31;9(9):716.
8. Dellière S, Aimanianda V. Humoral immunity against Aspergillus fumigatus. Mycopathologia. 2023 Oct;188(5):603-21.
9. Dabuo B, Xorlali N, Amoliga NT, Atibodu ZK, Newman PM, Mohammed A, Ali RA, Abudu A. Aspergillus and Aspergillosis in People with Chronic Diseases. Aspergillus and Aspergillosis-Advances in Genomics, Drug Development, Diagnosis and Treatment: Advances in Genomics, Drug Development, Diagnosis and Treatment. 2023 Nov 2:39.
10. Tiew PY, Thng KX, Chotirmall SH. Clinical Aspergillus signatures in COPD and bronchiectasis. Journal of Fungi. 2022 May 5;8(5):480.
11. Bao Z, Chen H, Zhou M, Shi G, Li Q, Wan H. Invasive pulmonary aspergillosis in patients with chronic obstructive pulmonary disease: a case report and review of the literature. Oncotarget. 2017 Apr 8;8(23):38069.
12. Gu Y, Ye X, Liu Y, Wang Y, Shen K, Zhong J, Chen B, Su X. A risk-predictive model for invasive pulmonary aspergillosis in patients with acute exacerbation of chronic obstructive pulmonary disease. Respiratory Research. 2021 Jun 9;22(1):176.
13. Upadhyay P, Wu CW, Pham A, Zeki AA, Royer CM, Kodavanti UP, Takeuchi M, Bayram H, Pinkerton KE. Animal models and mechanisms of tobacco smoke-induced chronic obstructive pulmonary disease (COPD). Journal of Toxicology and Environmental Health, Part B. 2023 Jul 4;26(5):275-305.
14. Chetambath R, Panicker V, editors. Clinical Allergy and Asthma Management in Adolescents and Young Adults. CRC Press; 2021 Nov 29.
15. Page ID, Byanyima R, Hosmane S, Onyachi N, Opira C, Richardson M, Sawyer R, Sharman A, Denning DW. Chronic pulmonary aspergillosis commonly complicates treated pulmonary tuberculosis with residual cavitation. European Respiratory Journal. 2019 Mar 18;53(3).
16. Agarwal R, Saxena P, Muthu V, Sehgal IS, Dhooria S, Prasad KT, Aggarwal AN, Chakrabarti A. Evaluation of simpler criteria for diagnosing allergic bronchopulmonary aspergillosis complicating asthma. Frontiers in Cellular and Infection Microbiology. 2022 Mar 25;12:861866.
17. Sunman B, Ademhan Tural D, Ozsezen B, Emiralioglu N, Yalcin E, Özçelik U. Current approach in the diagnosis and management of allergic bronchopulmonary aspergillosis in children with cystic fibrosis. Frontiers in Pediatrics. 2020 Oct 20;8:582964.
18. Agarwal R, Sehgal IS, Muthu V, Denning DW, Chakrabarti A, Soundappan K, Garg M, Rudramurthy SM, Dhooria S, Armstrong-James D, Asano K. Revised ISHAM-ABPA working group clinical practice guidelines for diagnosing, classifying and treating allergic bronchopulmonary aspergillosis/mycoses. European Respiratory Journal. 2024 Apr 4;63(4).
19. Shah A, Panjabi C. Allergic bronchopulmonary aspergillosis: a perplexing clinical entity. Allergy, asthma & immunology research. 2016 Jul 1;8(4):282-97.
20. Kwizera R, Bongomin F, Olum R, Worodria W, Bwanga F, Meya DB, Kirenga BJ, Gore R, Fowler SJ, Denning DW. Prevalence of Aspergillus fumigatus skin positivity in adults without an apparent/known atopic disease in Uganda. Therapeutic advances in infectious disease. 2021 Aug;8:20499361211039040.
21. Hedayati N, Mortezaee V, Mahdaviani SA, Mirenayat MS, Hassanzad M, Pourabdollah M, Heshmatnia J, Fakharian A, Pourdolat G, Sharifynia S, Vakili M. Prevalence of specific immunoglobulin E and G against Aspergillus fumigatus in patients with asthma. Current Medical Mycology. 2018 Dec;4(4):7.
22. Murugavel A, Ramakrishnan J. Virulence and pathogenicity of secondary fungal infections. Critical Reviews in Microbiology. 2026 Jan 2;52(1):139-58.
23. Shamly V, Kali A, Srirangaraj S, Umadevi S. Comparison of microscopic morphology of fungi using lactophenol cotton blue (LPCB), iodine glycerol and congo red formaldehyde staining. Journal of clinical and diagnostic research: JCDR. 2014 Jul 20;8(7):DL01.
24. Ponka D, Baddar F. Microscopic potassium hydroxide preparation. Canadian Family Physician. 2014 Jan 1;60(1):57-.
25. Machuca A, Milagres AM. Use of CAS-agar plate modified to study the effect of different variables on the siderophore production by Aspergillus. Letters in applied microbiology. 2003 Mar 1;36(3):177-81.
26. Taylor AW, Bruno RS, Frei B, Traber MG. Benefits of prolonged gradient separation for high-performance liquid chromatography–tandem mass spectrometry quantitation of plasma total 15-series F2-isoprostanes. Analytical biochemistry. 2006 Mar 1;350(1):41-51.
27. Laemmli UK. Cleavage of structural proteins during the assembly of the head of bacteriophage T4. nature. 1970 Aug 15;227(5259):680-5.
28. Brunelle JL, Green R. Coomassie blue staining. InMethods in enzymology 2014 Jan 1 (Vol. 541, pp. 161-167). Academic Press.
29. Li L, Zhang Y, Lv Y, Qu F, Ma Q. Emerging native Orbitrap mass spectrometry for probing higher-order structures of proteins: Recent progress and applications. TrAC Trends in Analytical Chemistry. 2024 Jan 1;170:117424.
30. Ekseth OK, Kuiper M, Mironov V. orthAgogue: an agile tool for the rapid prediction of orthology relations. Bioinformatics. 2014 Mar 1;30(5):734-6.
31. Saha S, Raghava GP. BcePred: prediction of continuous B-cell epitopes in antigenic sequences using physico-

ISSN: 0019-5138
DOI: https://doi.org/10.24321/0019.5138.202615

chemical properties. InInternational conference on artificial immune systems 2004 Sep 13 (pp. 197-204). Berlin, Heidelberg: Springer Berlin Heidelberg.
32. Vita R, Mahajan S, Overton JA, Dhanda SK, Martini S, Cantrell JR, Wheeler DK, Sette A, Peters B. The immune epitope database (IEDB): 2018 update. Nucleic acids research. 2019 Jan 8;47(D1):D339-43.
33. Dimitrov I, Bangov I, Flower DR, Doytchinova I. AllerTOP v. 2—a server for in silico prediction of allergens. Journal of molecular modeling. 2014 Jun;20(6):2278.
34. Verma S, Sugadev R, Kumar A, Chandna S, Ganju L, Bansal A. Multi-epitope DnaK peptide vaccine against S. Typhi: an in silico approach. Vaccine. 2018 Jun 27;36(28):4014-22.
35. Hoover DM, Wu Z, Tucker K, Lu W, Lubkowski J. Antimicrobial characterization of human β-defensin 3 derivatives. Antimicrobial agents and chemotherapy. 2003 Sep;47(9):2804-9.
36. Aslam S, Ahmad S, Noor F, Ashfaq UA, Shahid F, Rehman A, Tahir ul Qamar M, Alatawi EA, Alshabrmi FM, Allemailem KS. Designing a multi-epitope vaccine against chlamydia trachomatis by employing integrated core proteomics, immuno-informatics and in silico approaches. Biology. 2021 Oct 3;10(10):997.
37. Khalid K, Irum S, Ullah SR, Andleeb S. In-silico vaccine design based on a novel vaccine candidate against infections caused by Acinetobacter baumannii. International journal of peptide research and therapeutics. 2022 Jan;28(1):16.
38. Afshan G, Yaseen N, Ali SH, Khan AU. Immunoinformatics-Based development of a Multi-Epitope vaccine candidate targeting coinfection by Klebsiella pneumoniae and Acinetobacter baumannii. BMC Infectious Diseases. 2025 Jul 3;25(1):894.
39. Saha S, Raghava GP. Prediction of continuous B-cell epitopes in an antigen using recurrent neural network. Proteins: Structure, Function, and Bioinformatics. 2006 Oct 1;65(1):40-8.
40. Doytchinova IA, Flower DR. VaxiJen: a server for prediction of protective antigens, tumour antigens and subunit vaccines. BMC bioinformatics. 2007 Jan 5;8(1):4.
41. Li J, Ju Y, Jiang M, Li S, Yang XY. Epitope-based vaccines: the next generation of promising vaccines against bacterial infection. Vaccines. 2025 Feb 27;13(3):248.
42. Semple F, Webb S, Li HN, Patel HB, Perretti M, Jackson IJ, Gray M, Davidson DJ, Dorin JR. Human β-defensin 3 has immunosuppressive activity in vitro and in vivo. European journal of immunology. 2010 Apr;40(4):1073-8.
43. Wang Y, Kuan PJ, Xing C, Cronkhite JT, Torres F, Rosenblatt RL, DiMaio JM, Kinch LN, Grishin NV, Garcia CK. Genetic defects in surfactant protein A2 are associated with pulmonary fibrosis and lung cancer. The American Journal of Human Genetics. 2009 Jan 9;84(1):52-9.
44. Ocansey BK, Otoo B, Adjei A, Gbadamosi H, Kotey FC, Kosmidis C, Afriyie-Mensah JS, Denning DW, Opintan JA. Chronic pulmonary aspergillosis is common among patients with presumed tuberculosis relapse in Ghana. Medical Mycology. 2022 Sep;60(9):myac063.
45. Goh KJ, Yii A, Lapperre T, Chan A, Chew F, Chotirmall S, et al. Sensitization to Aspergillus species is associated with frequent exacerbations in severe asthma. J Asthma Allergy. 2017 Apr;Volume10:131–40.
46. Al-Saleh AA, Farid E, Makhlooq M, Mahdi M, Reda M, Zaid T, Al-Alawi S, Panjwani A, Salman N, Ali HR, Bindayna K. Allergic aspergillosis in asthmatic patients in a tertiary hospital in the Kingdom of Bahrain. Journal of laboratory physicians. 2019 Oct;11(4):373.
47. Otu A, Kosmidis C, Mathioudakis AG, Ibe C, Denning DW. The clinical spectrum of aspergillosis in chronic obstructive pulmonary disease. Infection. 2023 Aug;51(4):813-29.
48. Tong X, Cheng A, Xu H, Jin J, Yang Y, Zhu S, Li Y. Aspergillus fumigatus during COPD exacerbation: a pair-matched retrospective study. BMC pulmonary medicine. 2018 Apr 3;18(1):55.
49. Ortiz SC, Pennington K, Thomson DD, Bertuzzi M. Novel insights into Aspergillus fumigatus pathogenesis and host response from state-of-the-art imaging of host–pathogen interactions during infection. Journal of Fungi. 2022 Mar 4;8(3):264.
50. Ledoux MP, Herbrecht R. Invasive pulmonary aspergillosis. Journal of Fungi. 2023 Jan 17;9(2):131.
51. Martinez-Garcia MA, Miravitlles M. Bronchiectasis in COPD patients: more than a comorbidity?. International journal of chronic obstructive pulmonary disease. 2017 May 11:1401-11.
52. Bhalla AS, Goyal A, Guleria R, Gupta AK. Chest tuberculosis: Radiological review and imaging recommendations. Indian Journal of Radiology and Imaging. 2015 Jul;25(03):213-25.
53. Everaerts S, Janssens W, Dupont L, Vanaudenaerde B. Exploration of challenging phenotypes in Chronic Obstructive Pulmonary Disease: Aspergillus fumigatus, bronchiectasis and asthma-COPD overlap.
54. Amin R, Dupuis A, Aaron SD, Ratjen F. The effect of chronic infection with Aspergillus fumigatus on lung function and hospitalization in patients with cystic fibrosis. Chest. 2010 Jan 1;137(1):171-6.
55. Achilonu CC, Davies A, Kanu OO, Noel CB, Oladele R. Recent advances and future perspectives in mitigating invasive antifungal-resistant pathogen Aspergillus fumigatus in Africa. Current Treatment Options in Infectious Diseases. 2024 Mar;16(1):14-33.
56. Haas H. Fungal siderophore metabolism with a focus on Aspergillus fumigatus. Natural product reports. 2014;31(10):1266-76.

ISSN: 0019-5138
DOI: https://doi.org/10.24321/0019.5138.202615

57. Luptáková D, Patil RH, Dobiáš R, Stevens DA, Pluháček T, Palyzová A, Káňová M, Navrátil M, Vrba Z, Hubáček P, Havlíček V. Siderophore-based noninvasive differentiation of Aspergillus fumigatus colonization and invasion in pulmonary aspergillosis. Microbiology Spectrum. 2023 Apr 13;11(2):e04068-22.
58. Schrettl M, Bignell E, Kragl C, Sabiha Y, Loss O, Eisendle M, Wallner A, Arst Jr HN, Haynes K, Haas H. Distinct roles for intra-and extracellular siderophores during Aspergillus fumigatus infection. PLoS pathogens. 2007 Sep;3(9):e128.
59. Kang Y, Ma W, Li Q, Wang P, Jia W. Epidemiology, antifungal susceptibility and biological characteristics of clinical Aspergillus fumigatus in a tertiary hospital. Scientific Reports. 2025 May 15;15(1):16906.
60. Blachowicz A, Chiang AJ, Romsdahl J, Kalkum M, Wang CC, Venkateswaran K. Proteomic characterization of Aspergillus fumigatus isolated from air and surfaces of the International Space Station. Fungal Genetics and Biology. 2019 Mar 1;124:39-46.
61. Abou-Kandil A, Tröger-Görler S, Pschibul A, Krüger T, Rosin M, Schmidt F, Akbarimoghaddam P, Sarkar A, Cseresnyés Z, Shadkchan Y, Heinekamp T. The proteomic response of Aspergillus fumigatus to amphotericin B (AmB) reveals the involvement of the RTA-like protein RtaA in AmB resistance. MicroLife. 2025;6:uqae024.
62. Pinzan CF, Valero C, de Castro PA, da Silva JL, Earle K, Liu H, Horta MA, Kniemeyer O, Krüger T, Pschibul A, Cömert DN. Aspergillus fumigatus conidial surface-associated proteome reveals factors for fungal evasion and host immunity modulation. Nature microbiology. 2024 Oct;9(10):2710-26.
63. Vivek-Ananth RP, Mohanraj K, Vandanashree M, Jhingran A, Craig JP, Samal A. Comparative systems analysis of the secretome of the opportunistic pathogen Aspergillus fumigatus and other Aspergillus species. Scientific reports. 2018 Apr 26;8(1):6617.
64. Zuleta MC, Gómez OM, Misas E, Torres S, Rúa-Giraldo ÁL, McEwen JG, Garcia AM, Borges CL, Hernández O, López AM. Species identification and orthologous allergen prediction and expression in the genus Aspergillus. Journal of Fungi. 2025 Jan 27;11(2):98.
65. Shemesh E, Hanf B, Hagag S, Attias S, Shadkchan Y, Fichtman B, Harel A, Krüger T, Brakhage AA, Kniemeyer O, Osherov N. Phenotypic and Proteomic Analysis of the Aspergillus Fumigatus Δ prtt, Δ xprg and Δ xprg/Δ prtt Protease-Deficient Mutants. Frontiers in microbiology. 2017 Dec 12;8:2490.
66. Akhtar N, Singh A, Upadhyay AK, Mannan MA. Design of a multi-epitope vaccine against the pathogenic fungi Candida tropicalis using an in silico approach. Journal of Genetic Engineering and Biotechnology. 2022 Dec 1;20(1):140.
67. Choudhury A, Kumar P, Nafidi HA, Almaary KS, Wondmie GF, Kumar A, Bourhia M. Immunoinformatics approaches in developing a novel multi-epitope chimeric vaccine protective against Saprolegnia parasitica. Scientific Reports. 2024 Jan 27;14(1):2260.
68. Tarang S, Kesherwani V, LaTendresse B, Lindgren L, Rocha-Sanchez SM, Weston MD. In silico design of a multivalent vaccine against Candida albicans. Scientific Reports. 2020 Jan 23;10(1):1066.

ISSN: 0019-5138
DOI: https://doi.org/10.24321/0019.5138.202615